

Article

Assessment of Best Management Practices on Hydrology and Sediment Yield at Watershed Scale in Mississippi Using SWAT

Dipesh Nepal and Prem B. Parajuli * 

Department of Agricultural and Biological Engineering, Mississippi State University, Starkville, MS 39762, USA; dn590@msstate.edu

* Correspondence: pparajuli@abe.msstate.edu; Tel.: +1-(662)-325-7350

Abstract: The selection and execution of appropriate best management practices (BMPs) in critical areas of a watershed can effectively reduce sediment yield. Objectives of this research include developing a watershed-scale Soil and Water Assessment Tool (SWAT) model for the Big Sunflower River Watershed (BSRW), identifying high sediment yield areas using calibrated and validated model, and assessing the effects of various BMPs. The efficiency of three BMPs, grassed waterways (GWW), vegetative filter strips (VFS), and grade stabilization structures (GSS), and their combinations in reducing sediment yield, were investigated. The model performed well for streamflow (P-factor = 0.72–0.87; R-factor = 0.74–1.27; R^2 = 0.60–0.86; NSE = 0.60–0.86) and total suspended solids (TSS) (P-factor = 0.56–0.89; R-factor = 0.43–2.83; R^2 = 0.62–0.91; NSE = 0.38–0.91) during calibration and validation. The simulation of individual BMPs revealed that GWW showed the highest sediment yield reduction (up to 44%), followed by VFS (up to 38%) and GSS (up to 7%). Two BMPs' combinations showed that GSS and GWW had the largest sediment yield reduction potential (up to 47%) while VFS and GSS had the lowest potential (up to 42%). Similarly, a combination of all three BMPs reduced the sediment yield up to 50%. The findings of this study will aid in sustainable watershed management and will be valuable for watershed managers and planners.

Keywords: best management practices (BMPs); SWAT; flow; model; sediment yield; watershed



Citation: Nepal, D.; Parajuli, P.B. Assessment of Best Management Practices on Hydrology and Sediment Yield at Watershed Scale in Mississippi Using SWAT. *Agriculture* **2022**, *12*, 518. <https://doi.org/10.3390/agriculture12040518>

Academic Editor: Rabin Bhattacharai

Received: 7 March 2022

Accepted: 3 April 2022

Published: 6 April 2022

Publisher's Note: MDPI stays neutral with regard to jurisdictional claims in published maps and institutional affiliations.



Copyright: © 2022 by the authors. Licensee MDPI, Basel, Switzerland. This article is an open access article distributed under the terms and conditions of the Creative Commons Attribution (CC BY) license (<https://creativecommons.org/licenses/by/4.0/>).

1. Introduction

Soil and water quality deterioration due to erosion is a worldwide issue in agricultural areas, and severe erosion can lead to land becoming uncultivable [1]. Sediments, one of the agricultural non-point source (NPS) pollutants [2], along with its associated contamination, is a major cause of water quality degradation [3,4]. Increased sediment level in water bodies is widespread aquatic pollution, which has had a negative impact on fish health and the aquatic ecosystem [5,6]. Moreover, sediment is identified as a “sink” for a large number of chemicals that adversely affect aquatic life, avian species, wildlife, and humans [7]. Increased turbidity due to sediments reduces light penetration and limits aquatic life production [8]. Similarly, sedimentation is a serious issue in the operation and management of reservoirs designed for various purposes, including agricultural and drinking water storage, flood control, hydropower generation, and recreation [9].

Land use change from existing natural land covers caused by human activities such as urbanization and agricultural practices has a negative impact on soil and water quality, resulting in erosion, decreased groundwater recharge, increased surface runoff, and deteriorated water quality [10,11]. Agriculture is considered the major consumer of soil and water resources as well as a significant source of NPS pollution [12]. The pollutants related to agriculture are sediments, nutrients, and pesticides caused by agricultural activities such as crop rotation, tillage, fertilizer application, and so on. Soil erosion destroys around 10 million ha of agricultural land each year, limiting the amount of cropland available for global food production [13]. In addition, the sediments, nutrients, and pesticides generated from

agricultural areas are carried away by surface runoff to the nearest waterbodies, causing deterioration of water resources. Therefore, to control the transport of NPS contaminants into waterbodies and to avoid soil and nutrient loss from agricultural lands, a suitable and realistic management approach should be implemented. Other watersheds with similar hydrological and physical circumstances will benefit from this type of management approach as well.

The Big Sunflower River Watershed (BSRW), the study area under consideration, is an agricultural intensive watershed. The Big Sunflower River has been designated as “ephemeral”, which means it is unfit for aquatic life or human consumption and does not support fisheries’ resources [14]. The United States Environmental Protection Agency (USEPA) has classified Big Sunflower River as impaired under clean water act Section 303 (d) due to high levels of total suspended solids/sediments, nutrients, turbidity, and low dissolved oxygen [15], which eventually makes its way to Gulf of Mexico. Long-term river water quality can have a significant impact on the environmental characteristics of a bay and coastal water bodies [16]. Conventional tillage is the most common system for crop production in the Mississippi delta [17]. Conventional tillage-based agriculture has the disadvantage of increasing soil erosion rates [18]. Modeling and analysis of data revealed that existing sediment yields in the impaired reaches of BSRW is up to 10.5 metric tons/km²/day [19]. NPS pollution of sediments and nutrients is primarily caused by crop cultivation in BSRW, whereas NPS pollution of pathogen is mainly caused by livestock, urbanization, and wildlife [20]. The change in land use in the Mississippi River Alluvial Plain, where BSRW lies, has altered streamflow conditions. Research conducted by [21] evaluated changing land use patterns to assess changes in land use, crop yield, and irrigation from 1969 to 2017. According to the study, the amount of irrigated cropland has grown by 45,000 hectares on average across all study area counties and up to twelve folds in one county. Both surface and groundwater are utilized for irrigation, which has altered streamflow. Significant hydrologic changes, such as streamflow depletion and baseflow reduction, have been observed.

Conservation practices, also known as best management practices (BMPs), can help to prevent soil erosion and enhance water quality by lowering the sediments and other pollutants washed away from agricultural fields [22–24]. Different BMPs, such as cover crops, buffer strips, tailwater recovery ponds, constructed wetlands, conservation tillage, etc., have been found to reduce runoff and pollutants [25]. In BSRW, tailwater recovery ponds in agricultural land use have been found to reduce streamflow by 2 to 6%, sediment by 3 to 20%, and increase groundwater storage rate by 0 to 20% depending on the size of the pond [26]. BMPs are either structural or nonstructural practices [27]. Structural BMPs are natural or artificial structures built on the field, e.g., grade stabilization structures (GSS) whereas nonstructural BMPs are the practices within the agricultural areas, e.g., contour farming that helps to reduce sediments and other pollutants.

It is unrealistic to expect such management strategies to be implemented throughout a watershed. As a result, high priority areas should be identified in order to save time, money, and resources [28]. The hydrological models and remote sensing technology are useful in identifying the critical erosion prone areas of a watershed [29]. Soil and Water Assessment Tool (SWAT) is a hydrological model that could be used to assess the impact of BMPs on non-point source pollution and water supplies at high erosion prone areas within a watershed [30].

To analyze the influence of BMPs on water quality at the watershed scale, watershed managers depend on computer-based models [31]. Due to the ability of SWAT to simulate non-point source pollutants such as sediments and nutrients, as well as agricultural operations such as tillage, crop rotation, and so on, at a watershed scale, it has been used for BMP evaluation and watershed management in different parts of the world [12,23,32,33]. SWAT outperforms other watershed scale models due to its capacity to accommodate tillage practices and site specific dimensions of BMPs [34]. A study by [27] presents an optimization technique for determining the best combination of structural BMPs for achieving

treatment goals at a watershed scale. Using the SWAT model, [35] assessed the long-term effect of structural BMPs on sediment and phosphorus loads' reduction in two Black Creek sub-watersheds. Five BMP scenarios were simulated, including both structural and non-structural measures using SWAT for environmental and cost benefit evaluation [33]. The SWAT model was utilized to simulate structural BMPs to demonstrate that watershed subdivision-induced spatial resolution effects have a significant impact on the evaluation of BMPs [36]. However, in Mississippi's agriculturally intensive northwestern region, limited studies have looked at the effects of structural BMPs on soil erosion and hydrology. Some nonstructural and structural BMPs were evaluated previously, such as crop rotation, tillage management, tailwater recovery ponds, vegetative filter strips (VFS), etc. [12,26,37]. The evaluation of grassed waterways (GWW) and GSS has not been conducted in the watershed to quantify sediment yields. This study evaluated BMPs such as VFS, GSS, and GWW and their combinations to see if the water quality benefits of combining BMPs are much larger than the benefits of using them separately. The impact assessment of these BMPs can be a novel contribution to the BSRW, which is an agricultural watershed.

The study is based on the hypothesis that the SWAT watershed modeling can help identify the high priority areas with comparatively higher sediment yields, and that simulating BMPs on these areas can provide estimates of potential mitigation. According to the literature review, the SWAT model has been widely used in several studies to assess the effects of BMPs on sediments and NPS pollution in different parts of the world. There is still a need to implement the SWAT model under various climatic and geographic scenarios. The watersheds differ in their hydrological and physical characteristics, so the response to runoff and sediment transport varies as well. Implementing SWAT in various watersheds allows researchers to better understand the complex flow and transport mechanisms that occur under changing environmental conditions. In light of the preceding, this study aimed to fulfill the following objectives: (a) development of a watershed scale model, (b) calibration and validation of SWAT model for simulating flow and sediment load, (c) locating areas with comparatively higher sediment yield using calibrated and validated model (d) evaluation of the impacts of BMPs and their combinations on streamflow and sediment yields at watershed and sub-watershed levels to test the extent to which combining BMPs improves water quality as compared to using them individually.

2. Materials and Methods

2.1. Study Area

The present study is carried out in the BSRW (8326 km²) of the Mississippi River Alluvial Plain, also known as Mississippi Delta in northwestern Mississippi. It is located between 91°10'0" to 90°14'0" E longitude and 32°37'0" to 34°50'0" N latitude and lies within 11 counties, namely Coahoma, Tallahatchie, Desha, Bolivar, Sunflower, Leflore, Washington, Humphreys, Sharkey, Yazoo, and Issaquena. Figure 1 shows the location map of the BSRW. Agriculture is the most prevalent land use in the area, with cotton (6%), soybeans (63%), corn (11%), and rice (1%) as the most common crops, followed by forested wetlands (18%) and open water (1%) according to the classification of the land cover map for the year 2020 retrieved from United States Department of Agriculture (USDA), National Agricultural Statistics Service (NASS) [38]. The watershed area has low topographic relief with minimum and maximum elevations of 23 m and 71 m above mean sea level, respectively. Prime soil types in the area include Alligator, Forestdale, Dowling, Dundee, and Sharkey, which fall under soil groups C and D of Natural Resources Conservation Services (NRCS) and have high clay and silt percentages contributing to higher surface runoff and low permeability [39].

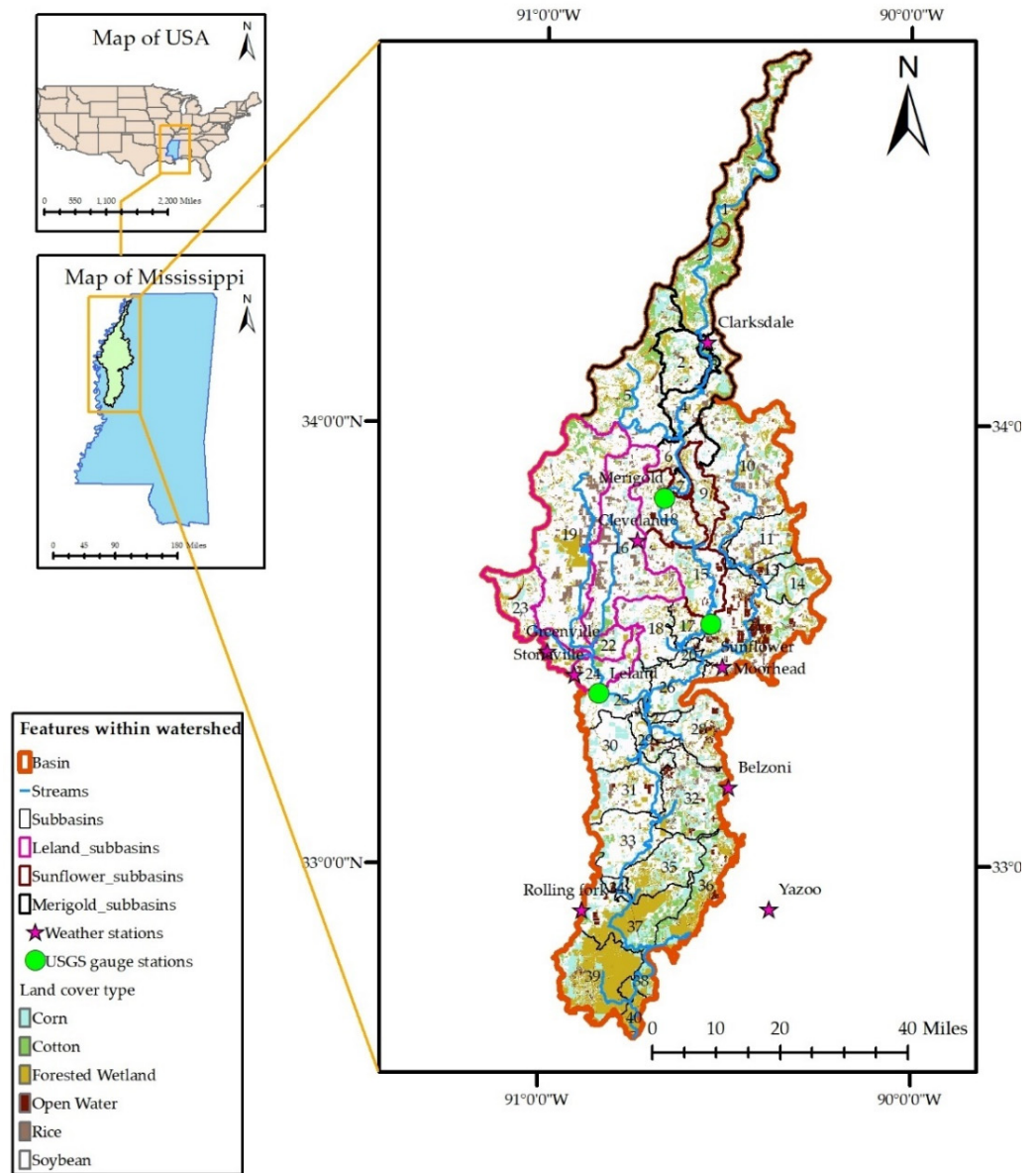


Figure 1. Location map of Big Sunflower River Watershed with landcover, weather stations, USGS gauge stations, streams, and subbasins.

2.2. SWAT Model

The SWAT is a continuous-time watershed scale model that requires a diversity of spatial and temporal information to run on a daily time step and is capable of evaluating the impacts of management on surface water, groundwater, and non-point source pollution in watersheds basins [30,40]. In SWAT, the simulation of hydrology is separated into land phase and water routing phase [41]. Figure 2 shows SWAT simulation flow chart. The SWAT delineates the watershed based on the provided digital elevation model (DEM), which is divided into several sub-basins and, further, into hydrological response units (HRUs) based on land use, soil, and slope class. This study used Arc SWAT 2012 as an ArcGIS 10.7 extension and interface for SWAT [42].

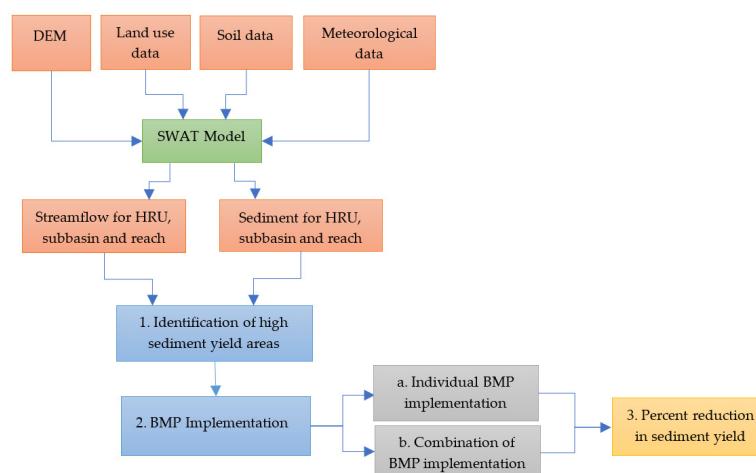


Figure 2. Flow chart showing SWAT methodology for runoff and sediment simulation.

The major driving force underlying all the processes in SWAT is water balance because it affects the sediments, nutrients, pesticides' transport, and plant growth [43]. Climatic conditions such as precipitation, air temperature, relative humidity, solar radiation, and wind speed control the water balance in the hydrologic cycle. When the temperature is below freezing, snow is calculated. Soil temperature is calculated because it influences the decay rate of residue in soil and water movement. SWAT simulates hydrologic processes such as precipitation, interception, surface runoff, infiltration, evapotranspiration, lateral subsurface flow, impoundments, tile drainage, water redistribution within soil profile, consumptive use by pumping, return flow, and deep aquifer recharge. SWAT simulates various types of land cover with a single plant growth model that distinguishes between perennial and annual plants and estimates nutrients and water removed from the root zone, biomass production, and transpiration. Sediment yield and erosion are calculated by the Modified Universal Soil Loss Equation (MUSLE) [44]. After the determination of water, nutrients, sediments, and pesticides' loadings from land phase, they are routed through the streams and reservoirs in the watershed [43].

SWAT Model Input

In the present study, BSRW is divided into 40 subbasins and 564 HRUs. The definition of HRUs was based on land use threshold, soil threshold, and slope threshold of 10% each. These threshold levels are determined by the project goal and the modeler's desired level of detail; land use threshold of 20%, soil threshold of 10%, and slope threshold of 20% is sufficient for most applications [45]. The primary inputs for the model are the DEM, land use land cover data, soil data, meteorological data, which includes precipitation, temperature, solar radiation, wind speed, and relative humidity. In addition, data for management practices, discharge, and sediment time series were obtained.

DEM of 30 m × 30 m resolution was downloaded from the United States Geological Survey website [46]. A DEM of 30 m resolution has been found adequate for streamflow and sediment simulation in different studies [47,48]. Cropland Data Layer (land cover data) of 30 m × 30 m resolution was obtained from the United States Department of Agriculture (USDA), National Agricultural Statistics Service (NASS) [38]. It was found that land cover resolution of 30 m gave an accurate estimation of streamflow [49,50]. The soil data was acquired from Natural Resources Conservation Service (NRCS) Soil Survey Geographic Database (SSURGO) database [51]. The temporal data on daily precipitation and daily temperature (2005–2020) were obtained from National Oceanic and Atmospheric Administration [52] for 8 weather stations, namely, Belzoni, Clarksdale, Cleveland, Moorhead, Rolling fork, Stoneville, Yazoo, and Greenville, based on maximum data availability. The available daily precipitation and temperature data were converted to SWAT readable .txt files with the help of the SWAT Weather Database tool [53]. Additional climate data on

solar radiation, wind speed, and relative humidity (2005–2020) were attained from Global weather data for SWAT [54]. Information on crop management operations, including the plant growing season, tillage, fertilization, pesticide application, irrigation, and harvest for four major crops, corn, cotton, soybean, and rice were obtained from MS Agricultural and Forestry Experiment Station variety trials annual reports [55]. Monthly streamflow data (2008–2017) were collected from [56] three USGS gauge stations, Merigold (USGS gauge: 07288280), Sunflower (USGS gauge: 07288500), and Leland (USGS gauge: 07288650) within the watershed. These gauge stations were chosen since they have the most data available from 2008 to 2017. For these stations, daily data for sediments was available biweekly from 2016 to 2018.

2.3. Model Calibration and Validation

Monthly calibration and validation of streamflow and TSS at subbasins 7 (Merigold), 15 (Sunflower), and 24 (Leland) were performed. An auto-calibration technique and sequential uncertainty fitting (SUFI-2) algorithm included in SWAT calibration and uncertainty procedures (SWAT-CUP) [57] were utilized to find a parameter set and values that give a satisfactory model performance in simulating streamflow and TSS. The SUFI-2 algorithm uses two statistics: P-factor and R-factor to quantify how well the observations are captured by the simulated 95 percent prediction uncertainty or 95 PPU band, which is calculated at the 2.5% and 97.5% levels. For a range of parameters, Latin hypercube sampling is done for 'n' times, where n is the number of simulations. Each time, the model gives a signal for each parameter. For every observation point, frequency distribution of discharge is obtained. From this frequency distribution, the cumulative distribution was calculated and the 95 PPU is the distance between the lower (2.5%) and the upper limit (97.5%) in the horizontal axis. For more information on 95PPU, the reader has to refer to the SWAT-CUP user manual [57]. P factor denotes the percentage of observed data captured by the 95 PPU envelope and ranges from 0 to 1, where 1 indicates a perfect fit. Similarly, the R factor is the thickness of the 95PPU band and is defined as the ratio of the average width of the 95PPU band to the standard deviation of the observed data. R factor ranges from 0 to infinity. The R factor of 0 and P factor of 1 is a condition where the simulation is exactly equal to the observed data. P factor of >0.7 and R factor of around 1 are suggested to be satisfactory for streamflow calibration, whereas a larger R factor and smaller P factor can be acceptable for sediment simulation [57]. In addition to the P factor and R factor, the comparison between the two signals simulated and observed data was evaluated using two statistical indicators, coefficient of determination (R^2) [58] and Nash–Sutcliffe efficiency (NSE) [59]. Global sensitivity analysis in SWAT-CUP gives values for t-statistic and p-value. T-statistic is the ratio of the coefficient of a parameter to its standard error and is a measure of sensitivity. p-value is a measure of the significance of a parameter. If the p-value is <0.05, the predictor is likely to have some effect on the response variable [57]. Therefore, a low p-value and high t-statistic suggested that the parameter was sensitive.

The model was calibrated from 2008 to 2012 and validated from 2013 to 2017 for observed monthly streamflow. The observed TSS concentration data were collected biweekly and there were 41 data points from 18 January 2016 to 11 February 2018. Therefore, to interpolate data into continuous daily data and to convert TSS concentration into loads, a USGS Load Estimator (LOADEST) [60] regression model was used. The interpolated continuous daily data were aggregated into monthly data for calibration and validation purposes.

To optimize the objective function, NSE in SWAT-CUP, the calibration procedure involved adjusting value ranges of 14 streamflow-related parameters in subbasins that are linked to the stations under consideration. Station Merigold was linked to subbasins 1, 2, 3, 4, 5, 6, 7; station Sunflower was linked to subbasins 8, 9, 15, and station Leland was linked to subbasins 16, 19, 22, 23, 24. This allowed for the incorporation of the spatial variability of the parameter values at different subbasins. These parameters used in streamflow calibration and sensitivity analysis are the initial Soil Conservation Service (SCS) curve number (CN2), the available water capacity of the soil layer (SOL_AWC), the soil evaporation

compensation factor (ESCO), Manning’s roughness coefficient (n) for the main channel (CH_N2), threshold water depth in shallow aquifer required for the occurrence of return flow (GWQMN), surface runoff lag coefficient (SURLAG), saturated hydraulic conductivity of soil layer (SOL_K), baseflow alpha factor (ALPHA_BF), groundwater delay time (GW_DELAY), groundwater “revap” coefficient (GW_REVAP), Manning’s roughness coefficient for overland flow (OV_N), average slope length (SLSUBBSN), slope length for lateral subsurface flow (SLSOIL) and snowfall temperature (SFTMP). The parameters used in sediment calibration are Universal Soil Loss Equation (USLE) equation support practice factor (USLE_P), peak rate adjustment factor for sediment routing in the main channel (PRF_BSN), channel erodibility factor (CH_COV1), channel cover factor (CH_COV2), monthly channel erodibility factor (CH_ERODMO), linear (SPCON) and exponent (SPEXP) parameters for calculating sediment re-entrained in channel sediment routing, average slope steepness (HRU_SLP), USLE soil erodibility factor (USLE_K), USLE crop cover factor (USLE_C), peak rate adjustment factor for sediment routing in the tributary channels (ADJ_PKR), and sediment concentration in lateral and groundwater flow (LAT_SED). These parameters for streamflow and sediment calibration were chosen from different literature based on their frequency of usage [43,61–63]. The range of values for the hydrologic parameters calibrated at the station Merigold and the parameters used in the sediment calibration are presented in the Tables 1 and 2 respectively.

Table 1. Parameters used in streamflow auto-calibration for Merigold station using SUFI-2.

Parameter Name	Subbasin	Fitted Value	Minimum Value	Maximum Value
R_CN2.mgt ^a	1, 2, 3, 4, 5, 6, 7	−0.07	−0.15	0.02
R_SOL_AWC(..).sol	1, 2, 3, 4, 5, 6, 7	−0.36	−0.50	0.07
V_ESCO.hru ^b	1, 2, 3, 4, 5, 6, 7	0.47	0.13	0.80
V_CH_N2.rte	1, 2, 3, 4, 5, 6, 7	0.01	0.00	0.01
V_GWQMN.gw	1, 2, 3, 4, 5, 6, 7	1623.37	795.84	3598.66
V_SURLAG.bsn	1, 2, 3, 4, 5, 6, 7	4.68	4.00	9.50
R_SOL_K(..).sol	1, 2, 3, 4, 5, 6, 7	−0.20	−0.24	0.27
V_ALPHA_BF.gw	1, 2, 3, 4, 5, 6, 7	0.74	0.44	0.81
V_GW_DELAY.gw	1, 2, 3, 4, 5, 6, 7	143.14	100.22	300.08
V_GW_REVAP.gw	1, 2, 3, 4, 5, 6, 7	0.08	0.00	0.13
V_OV_N.hru	1, 2, 3, 4, 5, 6, 7	0.22	0.20	0.36
R_SLSUBBSN.hru	1, 2, 3, 4, 5, 6, 7	−0.16	−0.20	0.09
R_SLSOIL.hru	1, 2, 3, 4, 5, 6, 7	0.48	0.18	0.50
V_SFTMP.bsn	1, 2, 3, 4, 5, 6, 7	−0.39	−5.00	0.77

^a R_ means multiplication by 1+ given value; ^b V_ means replacement of parameter value by the given value.

Table 2. Parameters used in TSS load auto-calibration using SUFI-2.

Parameter Name	Fitted Value	Minimum Value	Maximum Value
V_USLE_P.mgt ^a	0.62	0.50	0.70
V_PRF_BSN.bsn	0.13	0.10	0.20
V_CH_COV2.rte	0.18	0.15	0.19
V_CH_COV1.rte	0.01	0.00	0.10
V_CH_ERODMO(..).rte	0.12	0.00	0.15
V_SPCON.bsn	0.00	0.00	0.01
V_SPEXP.bsn	1.04	1.00	1.20
R_HRU_SLP.hru ^b	0.30	0.20	0.40
R_USLE_K(..).sol	−0.43	−0.50	−0.40
R_USLE_C{..}.plant.dat	−0.17	−0.20	−0.10
V_ADJ_PKR.bsn	1.59	1.50	1.70
V_LAT_SED.hru	1494.45	1400.00	1500.00

^a V_ means replacement of parameter value by the given value; ^b R_ means multiplication by 1+ given value.

2.4. LOADEST

Due to the cost of collection and limited resources, water quality samples are often collected less frequently than discharge. To convert biweekly TSS concentration data into continuous daily load data, a Load Estimator (LOADEST) statistical tool was used. LOADEST develops a regression model to estimate constituent loads in rivers and streams. The computation of the continuous TSS load is performed based on the relationship between streamflow and concentration data. The correlation between streamflow and water quality concentration data were determined using correlation coefficients [64]. It was found that the average correlation coefficients for sediment concentration data were 0.6, which was the highest among other water quality concentration data, such as phosphorous and nitrogen. The LOADEST regression model was applied to daily sediment data collected from 211 stations [64,65]. Estimates of annual sediment load were obtained with accuracy and precision with less than 10% error when the water quality data comprised 20 to 40% storm event (high flow) samples. LOADEST model has been implemented in a previous study to estimate and interpret suspended sediment loads, and other pollutant loads from the lower Boise River [66]. The model has been utilized to generate a rating curve of suspended sediment concentration based on the relationship between discharge and suspended sediment concentration in a watershed within Cape Bounty Arctic Watershed Observatory [67].

LOADEST is comprised of 11 regression models between daily discharge and water quality data. An automated model selection option can be invoked that helps to select the best regression model based on Akaike Information Criteria (AIC). As input, discrete water quality data and corresponding discharge data are written in calibration file “calib.inp” and continuous discharge data in estimation file “est.inp”. For model calibration, at least 12 water quality data are required. The statistical indicators, Adjusted Maximum Likelihood Estimation (AMLE), Maximum Likelihood Estimation (MLE), and Least Absolute Deviation (LAD) are used to calibrate and estimate within LOADEST. AMLE method assumes a normal distribution of model residuals, which is checked by a probability plot correlation coefficient (PPCC), where its value of 1 represents a perfect normal probability. More detailed information on the model can be found in the LOADEST user manual [60].

2.5. BMP Scenarios

Implementing BMPs at the watershed scale is time- and cost-demanding, so high-priority areas should be targeted [28]. This was performed by analyzing the average annual sediment yields from each subbasin. The BMPs, such as Vegetated filter strips (VFS), grade stabilization structures (GSS), grassed waterways (GWW), and all their combinations were simulated to evaluate the impact on streamflow and sediment yield at both watershed and sub-watershed levels. The adaptation of these BMPs was conducted in the agricultural areas of the watershed. The effectiveness of each BMP was assessed by applying it to the selected subbasins and evaluating the reduction of sediment yield at the subbasin and catchment scale. The effectiveness of their combinations was also determined and compared, resulting in a total of seven possibilities. Simulation of these scenarios was conducted by altering the SWAT model’s relevant parameter values and the sediment reduction from each scenario was analyzed. The calculation of sediment reduction is based on the following equation:

$$\text{Sediment reduction (\%)} = \frac{a - b}{a} \times 100 \quad (1)$$

where, a = sediment yield before BMP implementation, b = sediment yield after BMP implementation. The sediment yield before BMP implementation is the output of “Base Scenario”.

2.5.1. Grade Stabilization Structure

It is a structure made up of concrete, rock, earth, or steel installed on slopes of natural/artificial channels to stabilize grade, reduce erosion, and improve water quality [68].

The parameters, average slope of the main channel along the channel length (CH_S2), and channel erodibility factor (CH_ERODMO) were adjusted for the simulation of GSS.

2.5.2. Grassed Waterway

Adequately vegetated natural/artificial channels are established to transport concentrated flow at safe velocities, resulting in a reduction of surface erosion. The vegetation also helps to reduce nutrients through soil sorption, plant uptake, and absorption into sediment entrapments [68]. The GWW was simulated in SWAT by modifying the scheduled management operation (.ops) file, which involved parameters such as the flag for simulation of GWW (GWATI), Manning’s roughness coefficient for overland flow (GWATN), the linear parameter for calculating sediment in GWWs (GWATSPCON), depth of GWW channel from top to bottom of the bank (GWATD), average GWW width (GWATW), length of GWW (GWATL), and average slope of GWW channel (GWATS). The beginning of the simulation was assigned as the year, month, and day on which the operation takes place.

2.5.3. Vegetative Filter Strip

They are the vegetated areas between croplands, grazing lands, forestlands, and water bodies installed to filter out sediments and nutrients from the runoff water. The runoff water leaving a field is slowed down, which helps sediments to settle down and reduce nutrients through plant uptake and absorption into deposited sediments [68]. The effect of VFS in reducing sediment yield was assessed by adjusting parameters in the scheduled management operation (.ops) file (Table 3). These parameters include the flag for simulation (VFSI), ratio of field area to filter strip area (VFSRATIO), fraction of HRU draining to the most concentrated 10% of the VFS area (VFSCON), and fraction of flow within the most concentrated 10% of the fully channelized VFS (VFSCH). The year, month, and day on which the operation takes place were assigned as the start of the simulation.

Table 3. Simulation of BMPs in SWAT.

BMP Type	Parameters	Parameter Adjusted/Used	References
GSS	CH_S(2)	−0.00016 to 0.001752	[27,31,35,36]
	CH_ERODMO	0, representing nonerosive channel	
GWW	GWATI	1	[69,70]
	GWATN	0.35	
	GWATL	Default, 1000 km	[69–71]
	GWATW	10 m	
	GWATD	$3/64 \times \text{GWATW}$	[69]
	GWATS	$\text{HRU_SLP} \times 0.75$	[69–71]
GWATSPCON	Default, 0.005		
VFS	VFSI	1	[68,71,72]
	VFSRATIO	40	
	VFSCON	0.5	[68,73]
	VFSCH	0	

3. Results and Discussion

3.1. Flow Calibration and Validation

To evaluate the SWAT-CUP model performance, statistical parameters, P-factor, R-factor, R^2 , and NSE were used. Table 4 summarizes the statistics for streamflow calibration at all three stations. Figure 3 depicts the streamflow calibration from January 2008 to December 2012 and validation from January 2013 to December 2017 for the Merigold gauge station. P-factor of a value greater than 0.7 and R-factor of a value less than 1.5 for streamflow is adequate and these two parameters are used to assess the calibration and validation strength [32]. For watershed-scale models, the model performance for flow simulation has been found satisfactory if R^2 is greater than 0.6 and NSE is greater than 0.5 [74]. The NSE and R^2 statistics of streamflow were also compared to the previous studies

given in [75], which reviewed over 250 peer-reviewed published articles. The literature review suggested that these statistical indicators show reasonable accuracy.

Table 4. Evaluation of model performance during streamflow calibration and validation.

Station	Calibration				Validation			
	P-Factor	R-Factor	R ²	NSE	P-Factor	R-Factor	R ²	NSE
Merigold	0.87	0.87	0.75	0.74	0.79	0.85	0.60	0.60
Sunflower	0.77	0.74	0.78	0.76	0.85	0.85	0.86	0.86
Leland	0.72	0.81	0.71	0.70	0.80	1.27	0.82	0.81

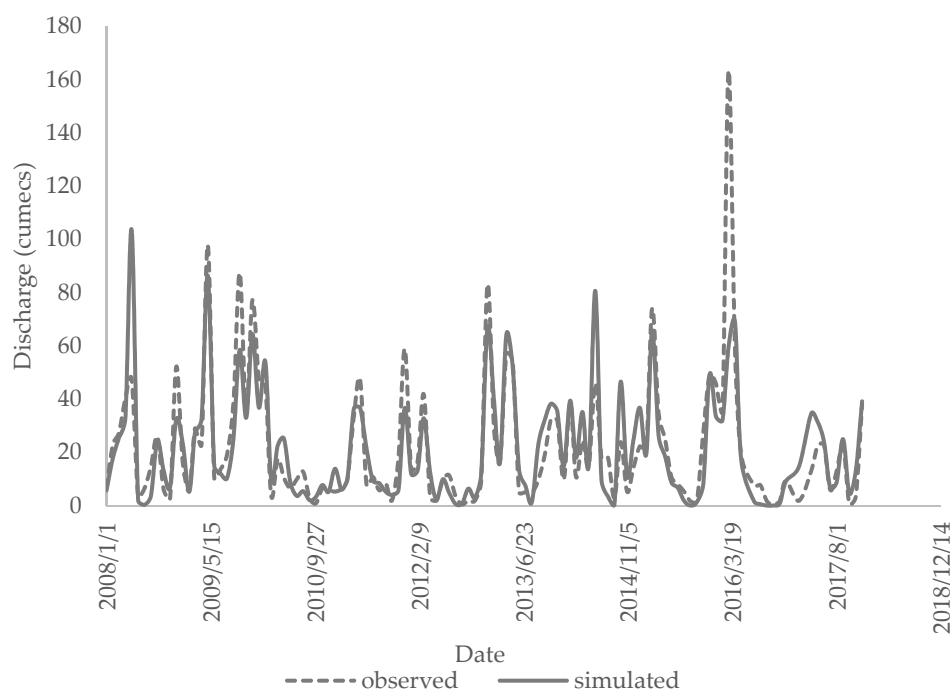


Figure 3. Observed and simulated monthly streamflow hydrographs during the calibration (2008–2012) and validation (2013–2017) periods for Merigold USGS gauge station.

3.2. Sediment Calibration and Validation

Table 5 summarizes the statistics for TSS load calibration and validation at all three USGS gauge stations. The observed and simulated sediment loads at Merigold gauge station were used for the calibration period between January 2016 to June 2017 and the validation period from July 2017 to December 2018 are shown in Figure 4. At the watershed scale, the model performance for sediment simulation has been found satisfactory if R² is greater than 0.40 and NSE is greater than 0.45 [74]. The values of R² and NSE obtained are comparable or better than that of prior sediment modeling studies. Monthly sediment load validation was determined NSE and R² of 0.11 and 0.19, respectively, in a study conducted at the Warner Creek watershed in Maryland [76]. However, the simulated annual sediment yield was in good agreement with the observed data. Lowest R² of up to 0.34 was obtained during sediment load verification in nine gauging station in a study conducted at Vistonis lagoon watershed in northern Greece, and SWAT was able to simulate the sediment transport correctly [77]. This study utilized rainfall data from eight ground weather stations, streamflow and bi-weekly TSS data from three USGS gauge stations. There may be a possible source of error here due to variability of rainfall data in the model performance. However, for the comparative assessment of BMPs, the model-simulated results provided good indicators.

Table 5. Evaluation of model performance during TSS load calibration and validation.

Station	Calibration				Validation			
	P-Factor	R-Factor	R ²	NSE	P-Factor	R-Factor	R ²	NSE
Merigold	0.72	0.82	0.77	0.70	0.72	1.35	0.62	0.61
Sunflower	0.89	0.87	0.91	0.91	0.56	0.43	0.66	0.38
Leland	0.72	0.88	0.90	0.85	0.61	2.83	0.80	0.77

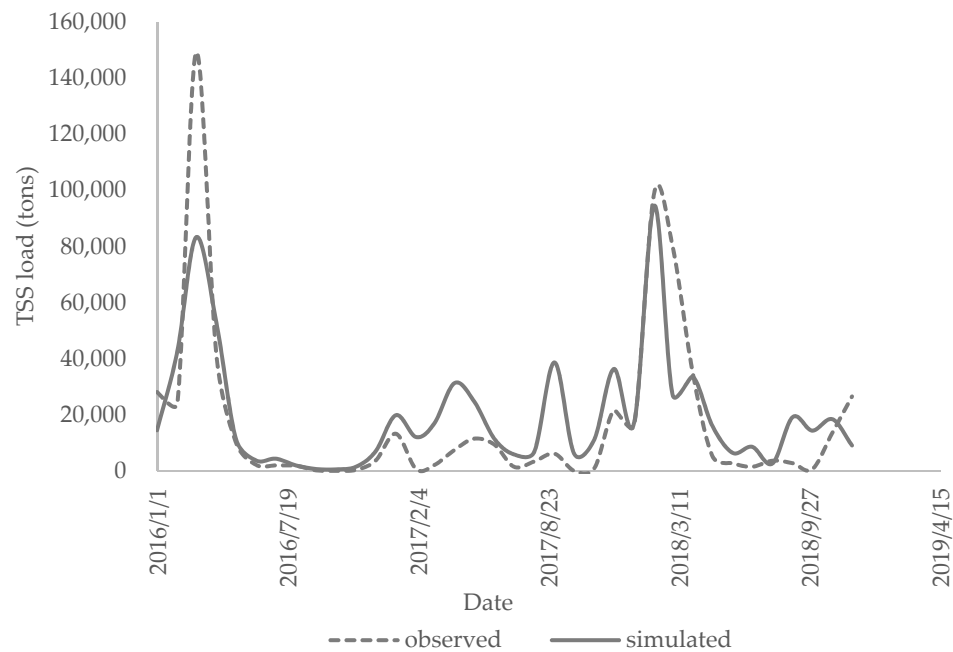


Figure 4. Comparison between observed and simulated monthly TSS load during the calibration (2016–2017) and validation (2017–2018) periods for Merigold USGS gauge station.

3.3. LOADEST Output

Continuous daily sediment load was generated using LOADEST from 1 January 2016 to 31 December 2018, which was then transformed into monthly sediment load. The LOADEST regression model’s ability to predict sediment loads of actual observed values is thought to be a good indicator of how well it functions on days when no samples were taken. The LOADEST model performance evaluation was conducted using load bias in percentage (Bp), NSE, and AMLE’s R². Table 6 shows the calibration results of the LOADEST model, suggesting good performance in the study area. The values of R² ranging from 0.90 to 0.96 and the values of NSE ranging from 0.50 to 0.92 for three stations show strong correlation. Bp ranging from −0.01% to 6.95% indicates positive bias with slight over prediction. The agreement between observed and estimated sediment load at all three stations indicated that the LOADEST model can be used to estimate the sediment load.

Table 6. Calibration results of regression models for TSS load at different stations.

Stations	Selected Model	PPCC ¹	R ²	NSE	Bp (%)
Merigold	$\text{Ln}(\text{Load}) = 11.59 + 1.17 \text{Ln}Q - 0.33 \text{Sin}(2 \pi \text{dtime}) + 0.31 \text{Cos}(2 \pi \text{dtime})^a$	0.97	0.91	0.92	6.95
Sunflower	$\text{Ln}(\text{Load}) = 11.94 + 1.18 \text{Ln}Q - 0.08 \text{Ln}Q^2 - 0.87 \text{Sin}(2 \pi \text{dtime}) + 0.33 \text{Cos}(2 \pi \text{dtime}) + 0.25 \text{dtime}$	0.99	0.90	0.77	2.96
Leland	$\text{Ln}(\text{Load}) = 11.08 + 1.21 \text{Ln}Q - 0.04 \text{Ln}Q^2 - 0.93 \text{Sin}(2 \pi \text{dtime}) + 0.27 \text{Cos}(2 \pi \text{dtime})$	0.98	0.96	0.50	−0.01

^a Ln (Load) = Natural log of calculated load (kg/d), LnQ = Ln (Q) – center of Ln (Q), where, Q is streamflow (ft³/s), dtime = decimal time – center of decimal time.

3.4. BMP Application Areas

To identify “high priority” areas within the watershed, the average annual sediment yield per unit area (tons/ha/year) from each subbasin from the year 2008 to 2020 was analyzed. Figure 5a shows the sediment yield from each subbasin in descending order, and the classification of subbasins based on sediment yield is shown in Figure 5b. There are four levels of classification: average annual sediment yield of 0 to 1 t/ha/year, 1 to 2 t/ha/year, 2 to 4 t/ha/year, and >4 t/ha/year. There are 16 subbasins that fall under the classification 0 to 1 t/ha/year, 13 that fall under the classification 1 to 2 t/ha/year, 5 that fall under the classification 2 to 4 t/ha/year, and 6 that fall under the classification >4 t/ha/year. The implementation of BMPs was carried out in the subbasins where sediment yield was greater than 1 ton/ha/year. This means that the BMPs were simulated in 24 subbasins (subbasins 1, 2, 3, 4, 5, 6, 7, 9, 10, 11, 12, 13, 14, 18, 20, 21, 26, 28, 30, 32, 34, 35, 36, 39) out of 40. The simulated average annual sediment yield of the watershed area was approximately 9 MT/year and these 24 subbasins contributed to 40% of it.

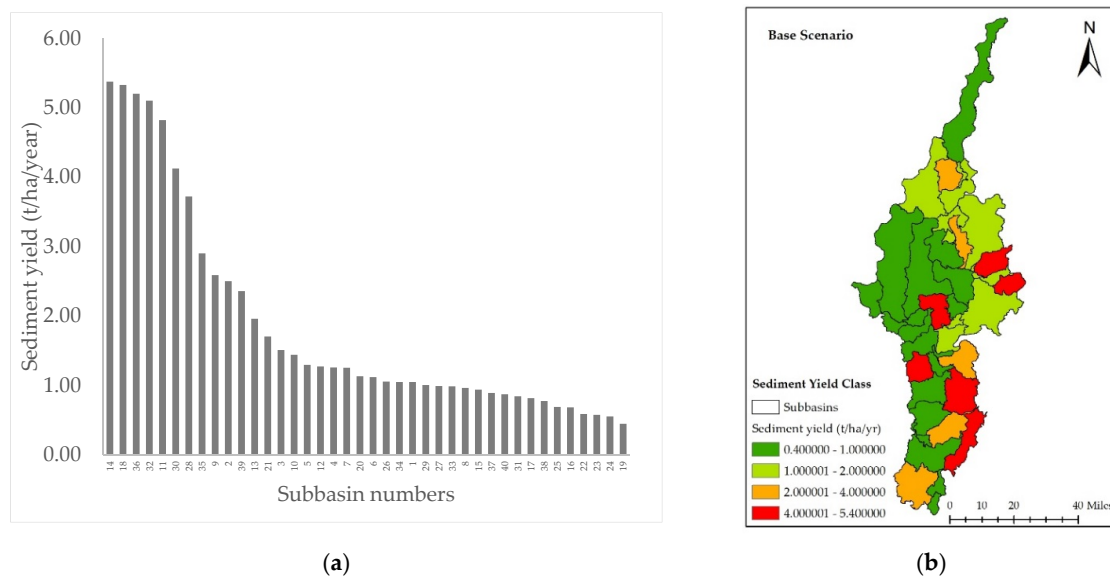


Figure 5. (a) Model simulated sediment yield from sub-basins in descending order; (b) subbasins classified according to average annual sediment yield per unit area.

3.5. Impacts of BMPs on Flow and Sediment Yield

The simulation results of sediment yield reduction at watershed and sub-watershed levels are summarized in Table 7 below.

Table 7. Effects of BMPs on sediment yield reduction at watershed and sub-watershed levels.

Scenarios	BMPs Sets	Average Annual Sediment Yield Reduction (%)	
		At Watershed Level	At Sub-Watershed Level (Average from All High Priority Subbasins)
Individual BMPs	GSS	7	5
	VFS	25	38
	GWW	30	44
Combination of 2 BMPs	VFS + GSS	30	42
	VFS + GWW	32	46
	GSS + GWW	35	47
Combination of 3 BMPs	VFS + GSS + GWW	36	50

3.5.1. Impacts of BMPs at the Watershed Level

The model outputs of average annual sediment yield and average annual streamflow from the year 2008 to 2020 were evaluated at the watershed level. The simulation results of individual BMPs, combinations of 2 BMPs, and a combination of all 3 BMPs indicate that they resulted in low to no flow reduction and significant sediment yield reduction (Figure 6). In the evaluation of individual BMPs' simulation, the GSS reduced flow by less than 1% and sediment yield by 7%. The VFS was able to reduce sediment yield by 25% but had no effect on flow. The GWW did not affect flow but reduced sediment yield by 30%.

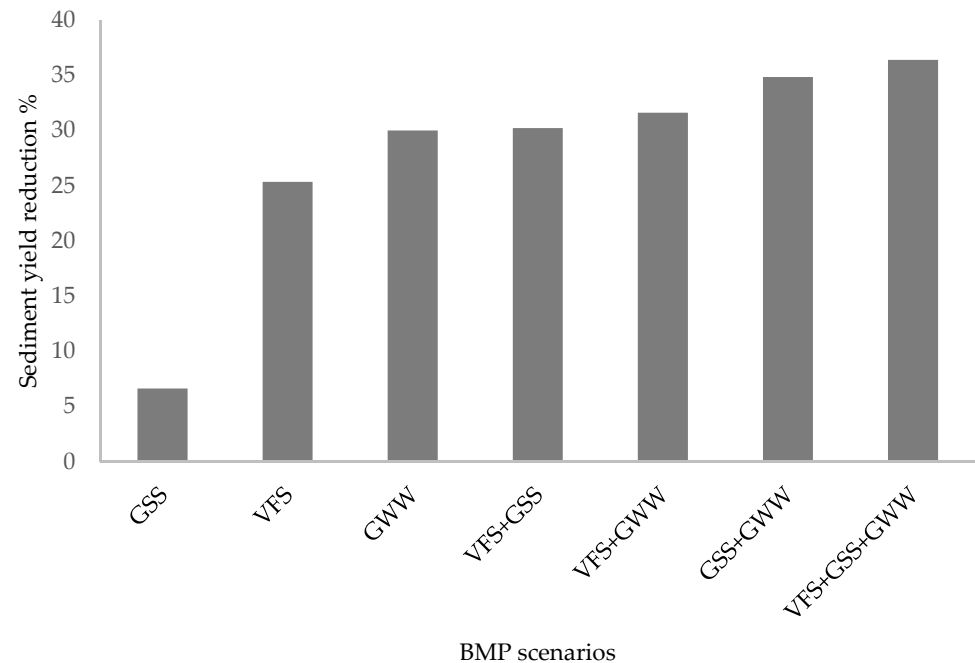


Figure 6. Average annual sediment yield reduction for different BMP scenarios at the watershed level.

Similarly, combinations of two BMPs were simulated, and average annual sediment yield was analyzed. The combination of VFS and GSS was able to reduce sediment yield by 30% and had a negligible reduction of streamflow of less than 1%. The combination of VFS and GWW reduced sediment yield by 32% and did not affect streamflow. A reduction of 35% on average annual sediment yield and less than 1% on average annual flow was attained by the combination of GSS and GWW. The combination of all three BMPs, VFS, GSS, and GWW reduced average annual sediment yield by 36% and average annual streamflow by less than 1%.

3.5.2. Impacts of BMPs at the Sub-Watershed Level

The simulation results of average annual sediment yield and average annual streamflow (2008–2020) for all the seven BMP scenarios were evaluated at the individual high priority subbasins. Figure 7 shows the range and mean of sediment yield reduction for each BMP scenario.

The GSS reduced flow by less than 1% at the subbasins. Less than 1% sediment yield reduction was observed at subbasin 9 and maximum sediment yield reduction of 23% was observed in subbasin 28. The average sediment yield reduction by GSS from all the high priority subbasins is 5%. VFS reduced sediment yield by a minimum of 10% to a maximum of 67% at subbasins 39 and 9, respectively, and the average sediment reduction was 38%. No effect on flow was observed. The GWW reduced sediment yield from 13% to 81%, minimum reduction at subbasin 39 and maximum reduction at subbasin 18, and an average reduction of 44%. There was no effect on flow.

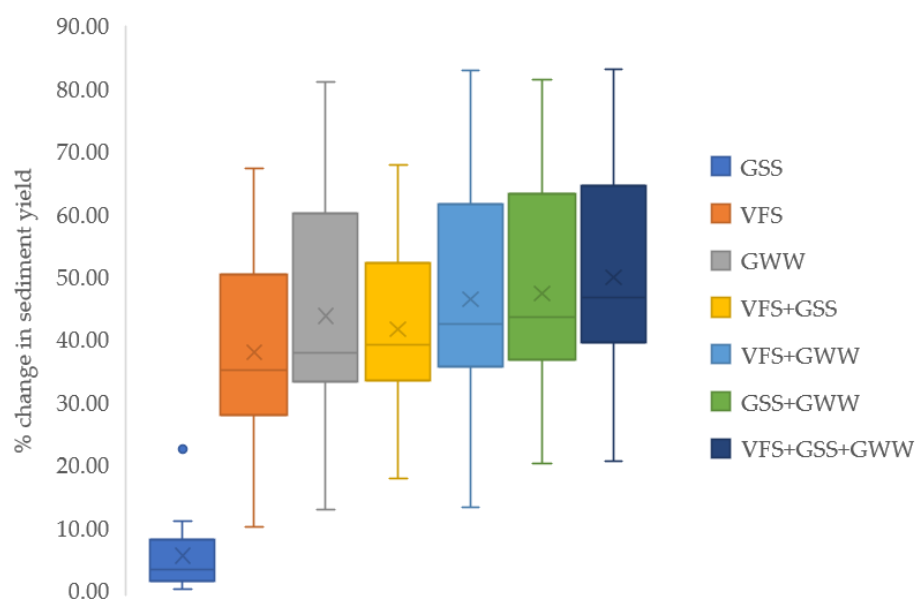


Figure 7. Side-by-side box plot comparing sediment yield reduction range at the sub-watershed level for different scenarios.

The combination of two BMPs, VFS + GSS, reduced flow by less than 1% and sediment yield by a minimum of 18% at subbasin 39 and a maximum of 68% at subbasin 18 with an average reduction of 42%. Similarly, VFS + GWW reduced sediment yield by 13% to 83% with an average of 46%; the minimum and maximum reduction were observed at subbasins 39 and 18, respectively. GSS + GWW reduced sediment yield by a minimum of 20% at subbasin 39 and a maximum of 81% at subbasin 18 with an average reduction of 47%. VFS + GWW and GSS + GWW had zero and less than 1% reduction in streamflow, respectively.

The combination of all three BMPs, VFS + GSS + GWW, could reduce the average annual sediment yield by a minimum of 21% at subbasin 39 and a maximum of 83% at subbasin 18. The average reduction from all the high priority subbasins under consideration was observed to be 50%.

3.5.3. Comparison of Results with Previous Studies

Higher sediment yield reductions were observed at the sub-watershed level compared to the watershed level, which is consistent with the findings of previous studies [71,78]. No effect on flow was observed for GWW and VFS at the watershed and sub-watershed levels. This is in accordance with the results obtained in other literature [35,71,79]. This has been attributed to the fact that VFS and GWW are typically designed to address sediment and nutrients, and the SCS curve number method determines the runoff simulation in SWAT, which is based on soil type and land cover rather than management operations. Slight reduction in flow (<1%) was observed for GSS. This is due to its impoundment effect. The structure's depth was set at 80% of the channel depth. Greater reduction in flow could be achieved with increased height of the structure.

GSS reduced less than 1% to a maximum of 23% sediment yield. Previous research conducted by [31] on the effect of GSS revealed that sediment reduction depends on the installation within channels of various class. There was no sediment reduction when GSS was installed within class 1 channels (channels originating from upland areas with no upstream channels). The highest sediment reduction of 74% was obtained when installed within class 4 streams (highest stream class located at very downstream of watershed). Implementation of GSS within class 2 and class 3 (classes between 1 and 4) resulted in sediment yield reduction of 2% and 9%, respectively. In addition, the GSS height used was 1.2 m. The height of the structure employed in the study has a variable height of 80% of the channel depth [70]. Therefore, the highest sediment reduction benefit was underestimated.

VFS was able to reduce 38% of sediment yields at sub-watershed level. A previous study found that for a width of 5 m to 35 m, the sediment yield reduction increased logarithmically from about 38% to 65% [80]. In another study by [81], VFS reduced sediment by up to 35%.

Similarly, GWW reduced 13% to 81% of sediment yield at the sub-watersheds. In a previous study by [71], GWW was able to reduce average annual sediment yield up to 79% at the sub-watershed scale and 14% at watershed scale. In another study by [82] the maximum reduction of average annual sediment at sub-watershed level was 85%. The maximum water quality benefit could be obtained from GWW rather than the combination VFS + GSS. Similarly, the combinations VFS + GWW and GSS + GWW outperformed GWW, but the difference in sediment reduction was not significant. Therefore, the implementation of GWW only could be conducted according to the need of sediment reduction.

The GWW had the maximum sediment reduction potential followed by VFS. Six different BMPs were simulated by [71], such as ponds, wetlands, cover crops, VFS, GWW, forage, and biomass planting, which found GWW to be the most effective BMP in reducing sediment and nutrient loads. GWW and VFS have been documented as the most effective BMPs in reducing sediments and nutrients from agricultural watersheds compared to GSS, detention ponds, and parallel terraces [27]. This can be attributed to the entrapment of sediments by slowing down the runoff due to vegetated cover [68].

4. Conclusions

This study was conducted in a watershed in northwestern Mississippi using a calibrated and validated SWAT model to simulate the runoff and sediment yield. The statistical indicators showed acceptable model performance in simulating the runoff and TSS load. LOADEST tool was used to interpolate continuous daily data of TSS load. Seven different structural BMP scenarios, GSS, GWW, VFS, and their combinations were implemented in the high priority areas within the watershed, and their impacts on flow and sediment yield reduction at both watershed and sub-watershed levels were documented.

The outcomes of the simulation revealed that all the selected BMPs had a substantial impact on sediment yield reduction and a 0 to less than 1% reduction in flow. The sediment yield reduction potential of different BMPs scenarios was variable, with the highest reduction in the case of a combination of all three BMPs. In the evaluation of individual BMPs, at both watershed and sub-watershed levels, GWW exhibited the highest sediment yield potential, followed by VFS, which explains their widespread use [71]. The combination of GSS and GWW had the highest potential for reducing sediment yield when compared to other combinations of two BMPs. According to the results, combining all three BMPs is the most preferable. However, in the event of budget limits, the combination of GSS and GWW could be utilized.

The findings of this study are beneficial to watershed managers as well as the scientific community. Watershed managers and decision-makers can make use of the information to help them choose appropriate BMPs and ensure sustainable watershed management. The findings of this work will aid modelers in successfully performing multisite SWAT calibration and validation using tools such as SWAT CUP and LOADEST.

It is worth noting that this study has not considered the costs, operation, maintenance, and life cycle of the BMPs. The technical efficacy of these approaches may be limited by local constraints such as geographic challenges, farmers' acceptance, resources availability, economic expenses, and so on. Future studies could help to analyze the uncertainty and fill this gap in the execution of the proposed BMPs at a watershed scale.

Author Contributions: Model development, run, analysis, and writing manuscript draft by D.N.; and supervision, manuscript review, editing, and funding acquisition by P.B.P. All authors have read and agreed to the published version of the manuscript.

Funding: This research was partially funded by USDA/NIFA-AFRI grant award # 2017-67020-26375.

Institutional Review Board Statement: Not applicable.

Informed Consent Statement: Not applicable.

Data Availability Statement: Not applicable.

Acknowledgments: Authors would like to acknowledge the partial financial support from AFRI competitive grant award # 2017-67020-26375 from the USDA/NIFA for this project. Authors wish to acknowledge United States Geological Survey (USGS) and all other collaborators for their support for this study.

Conflicts of Interest: The authors declare no conflict of interest.

References

1. Iowa State University Extension and Outreach. Soil Erosion: An Agricultural Production Challenge. Available online: <https://crops.extension.iastate.edu/encyclopedia/soil-erosion-agricultural-production-challenge> (accessed on 3 March 2022).
2. Ritter, W.F.; Shirmohammadi, A. *Agricultural Nonpoint Source Pollution: Watershed Management and Hydrology*; CRC Press: Boca Raton, FL, USA, 2000; pp. 1–2.
3. Wear, L.R.; Aust, W.M.; Bolding, M.C.; Strahm, B.D.; Dolloff, C.A. Effectiveness of best management practices for sediment reduction at operational forest stream crossings. *For. Ecol. Manag.* **2013**, *289*, 551–561. [[CrossRef](#)]
4. US EPA. 2000 National Water Quality Inventory Report to Congress. Available online: <https://www.epa.gov/waterdata/2000-national-water-quality-inventory-report-congress> (accessed on 3 March 2022).
5. Yuan, Y.; Dabney, S.M.; Bingner, R.L. Cost effectiveness of agricultural BMPs for sediment reduction in the Mississippi delta. *J. Soil Water Conserv.* **2002**, *57*, 259–267.
6. Donohue, I.; Garcia Molinos, J. Impacts of increased sediment loads on the ecology of lakes. *Biol. Rev.* **2009**, *84*, 517–531. [[CrossRef](#)] [[PubMed](#)]
7. Adams, W.J.; Kimerle, R.A.; Barnett, J.W., Jr. Sediment quality and aquatic life assessment. *Environ. Sci. Technol.* **1992**, *26*, 1864–1875. [[CrossRef](#)]
8. Affandi, F.A.; Ishak, M.Y. Impacts of Suspended sediment and metal pollution from mining activities on riverine fish population—A review. *Environ. Sci. Pollut. Res.* **2019**, *26*, 16939–16951. [[CrossRef](#)]
9. Moslemzadeh, M.; Roueinian, K.; Salarijazi, M. Improving the Estimation of sedimentation in multi-purpose dam reservoirs, considering hydrography and time scale classification of sediment rating curve (Case Study: Dez Dam). *Arab. J. Geosci.* **2022**, *15*, 256. [[CrossRef](#)]
10. Chen, J.; Theller, L.; Gitau, M.W.; Engel, B.A.; Harbor, J.M. Urbanization Impacts on surface runoff of the contiguous United States. *J. Environ. Manag.* **2016**, *187*, 470–481. [[CrossRef](#)]
11. Wang, R.; Kalin, L.; Kuang, W.; Tian, H. Individual and combined effects of land use/cover and climate change on wolf bay watershed streamflow in Southern Alabama. *Hydrol. Process.* **2014**, *28*, 5530–5546. [[CrossRef](#)]
12. Parajuli, P.B.; Jayakody, P.; Sassenrath, G.F.; Ouyang, Y.; Pote, J.W. Assessing the impacts of crop-rotation and tillage on crop yields and sediment yield using a modeling approach. *Agric. Water Manag.* **2013**, *119*, 32–42. [[CrossRef](#)]
13. Pimentel, D.; Burgess, M. Soil erosion threatens food production. *Agriculture* **2013**, *3*, 443–463. [[CrossRef](#)]
14. MDEQ. Basins and Streams—MDEQ. Available online: <https://www.mdeq.ms.gov/water/surface-water/watershed-management/water-quality-standards/basins-and-streams/> (accessed on 23 March 2022).
15. US EPA. Clean Water Act Section 303(d): Impaired Waters and Total Maximum Daily Loads (TMDLs). Available online: <https://www.epa.gov/tmdl> (accessed on 23 March 2022).
16. Kousali, M.; Salarijazi, M.; Ghorbani, K. Estimation of non-stationary behavior in annual and seasonal surface freshwater volume discharged into the Gorgan Bay, Iran. *Nat. Resour. Res.* **2022**, *31*, 835–847. [[CrossRef](#)]
17. Mississippi Agricultural & Forestry Experiment Station (MAFES). B1143 Current Agricultural Practices of the Mississippi Delta. Available online: <https://www.mafes.msstate.edu/publications/bulletins/b1143.pdf> (accessed on 23 March 2022).
18. Montgomery, D.R. Soil erosion and agricultural sustainability. *Proc. Natl. Acad. Sci. USA* **2007**, *104*, 13268–13272. [[CrossRef](#)] [[PubMed](#)]
19. MDEQ. TMDL for Organic Enrichment, Nutrients and Sediment for the Big Sunflower River. Available online: https://www.mdeq.ms.gov/wp-content/uploads/TMDLs/Yazoo/Big_Sunflower_River_FINAL_Organic_Enrichment_Nutrients_and_Sediment_TMDL.pdf (accessed on 23 March 2022).
20. MDEQ. Fecal Coliform TMDL for the Big Sunflower River Prefixes for Fractions and Multiples of SI Units. Available online: https://www.mdeq.ms.gov/wp-content/uploads/2017/06/BSR_and_LSR_DRAFT_Fecal_Coliform_TMDL.pdf (accessed on 23 March 2022).
21. Yasarer, L.M.W.; Taylor, J.M.; Rigby, J.R.; Locke, M.A. Trends in land use, irrigation, and streamflow alteration in the Mississippi River alluvial plain. *Front. Environ. Sci.* **2020**, *8*, 66. [[CrossRef](#)]
22. Mwangi, J.K.; Shisanya, C.A.; Gathenya, J.M.; Namirembe, S.; Moriasi, D.N. A modeling approach to evaluate the impact of conservation practices on water and sediment yield in Sasumua Watershed, Kenya. *J. Soil Water Conserv.* **2015**, *70*, 75–90. [[CrossRef](#)]

23. Himanshu, S.K.; Pandey, A.; Yadav, B.; Gupta, A. Evaluation of best management practices for sediment and nutrient loss control using SWAT model. *Soil Tillage Res.* **2019**, *192*, 42–58. [[CrossRef](#)]
24. Lam, Q.D.; Schmalz, B.; Fohrer, N. The impact of agricultural best management practices on water quality in a North German lowland catchment. *Environ. Monit. Assess.* **2011**, *183*, 351–379. [[CrossRef](#)]
25. Liu, Y.; Engel, B.A.; Flanagan, D.C.; Gitau, M.W.; McMillan, S.K.; Chaubey, I. A Review on Effectiveness of best management practices in improving hydrology and water quality: Needs and opportunities. *Sci. Total Environ.* **2017**, *601*, 580–593. [[CrossRef](#)]
26. Ni, X.; Parajuli, P.B. Evaluation of the impacts of BMPs and Tailwater recovery system on surface and groundwater using satellite imagery and SWAT reservoir function. *Agric. Water Manag.* **2018**, *210*, 78–87. [[CrossRef](#)]
27. Kaini, P.; Artita, K.; Nicklow, J.W. Optimizing structural best management practices using SWAT and genetic algorithm to improve water quality goals. *Water Resour. Manag.* **2012**, *26*, 1827–1845. [[CrossRef](#)]
28. Lamba, J.; Thompson, A.M.; Karthikeyan, K.G.; Panuska, J.C.; Good, L.W. Effect of best management practice implementation on sediment and phosphorus load reductions at subwatershed and watershed scale using SWAT model. *Int. J. Sedim. Res.* **2016**, *31*, 386–394. [[CrossRef](#)]
29. Pandey, A.; Chowdary, V.M.; Mal, B.C. Identification of critical erosion prone areas in the small agricultural watershed using USLE, GIS and remote sensing. *Water Resour. Manag.* **2007**, *21*, 729–746. [[CrossRef](#)]
30. Arnold, J.G.; Srinivasan, R.; Muttiah, R.S.; Williams, J.R. Large area hydrologic modeling and assessment part I: Model development 1. *J. Am. Water Resour. Assoc.* **1998**, *34*, 73–89. [[CrossRef](#)]
31. Arabi, M.; Frankenberger, J.R.; Engel, B.A.; Arnold, J.G. Representation of agricultural conservation practices with SWAT. *Hydrol. Process. Int. J.* **2008**, *22*, 3042–3055. [[CrossRef](#)]
32. Abbaspour, K.C.; Rouholahnejad, E.; Vaghefi, S.; Srinivasan, R.; Yang, H.; Klöve, B. A Continental-Scale hydrology and water quality model for Europe: Calibration and uncertainty of a high-resolution large-scale SWAT model. *J. Hydrol.* **2015**, *524*, 733–752. [[CrossRef](#)]
33. Ding, Y.; Dong, F.; Zhao, J.; Peng, W.; Chen, Q.; Ma, B. Non-point source pollution simulation and best management practices analysis based on control units in Northern China. *Int. J. Environ. Res. Public Health* **2020**, *17*, 868. [[CrossRef](#)]
34. Xie, H.; Chen, L.; Shen, Z. Assessment of agricultural best management practices using models: Current issues and future perspectives. *Water* **2015**, *7*, 1088–1108. [[CrossRef](#)]
35. Bracmort, K.S.; Arabi, M.; Frankenberger, J.R.; Engel, B.A.; Arnold, J.G. Modeling long-term water quality impact of structural BMPs. *Trans. ASABE* **2006**, *49*, 367–374. [[CrossRef](#)]
36. Arabi, M.; Govindaraju, R.S.; Hantush, M.M.; Engel, B.A. Role of watershed subdivision on modeling the effectiveness of best management practices with SWAT 1. *J. Am. Water Resour. Assoc.* **2006**, *42*, 513–528. [[CrossRef](#)]
37. Risal, A.; Parajuli, P.B.; Ouyang, Y. Impact of BMPs on water quality: A case study in big sunflower river watershed, Mississippi. *Int. J. River Basin Manag.* **2021**, 1–14. [[CrossRef](#)]
38. USDA. CropScape—NASS CDL Program. Available online: <https://nassgeodata.gmu.edu/CropScape/> (accessed on 29 January 2021).
39. Dakhllalla, A.O.; Parajuli, P.B.; Ouyang, Y.; Schmitz, D.W. Evaluating the Impacts of crop rotations on groundwater storage and recharge in an agricultural watershed. *Agric. Water Manag.* **2016**, *163*, 332–343. [[CrossRef](#)]
40. Arnold, J.G.; Kiniry, J.R.; Srinivasan, R.; Williams, J.R.; Haney, E.B.; Neitsch, S.L. *Input/Output Documentation; Soil Water Assessment Tool; Texas Water Resources Institute: College Station, TX, USA, 2012.* Available online: <https://swat.tamu.edu/media/69296/swat-iodocumentation-2012.pdf> (accessed on 5 March 2022).
41. Neitsch, S.L.; Arnold, J.G.; Kiniry, J.R.; Williams, J.R. *Soil and Water Assessment Tool Theoretical Documentation Version 2009; Texas Water Resources Institute: College Station, TX, USA, 2011; pp. 1–23.*
42. Soil & Water Assessment Tool. Available online: <https://swat.tamu.edu/software/arcsWat/> (accessed on 5 March 2022).
43. Arnold, J.G.; Moriasi, D.N.; Gassman, P.W.; Abbaspour, K.C.; White, M.J.; Srinivasan, R.; Santhi, C.; Harmel, R.D.; Van Griensven, A.; Van Liew, M.W. SWAT: Model use, calibration, and validation. *Trans. ASABE* **2012**, *55*, 1491–1508. [[CrossRef](#)]
44. Williams, J.R.; Berndt, H.D. Sediment yield prediction based on watershed hydrology. *Trans. ASAE* **1977**, *20*, 1100–1104. [[CrossRef](#)]
45. Winchell, M.; Srinivasan, R.; Di Luzio, M.; Arnold, J. *ArcSWAT Interface for SWAT 2005. User's Guide; Blackland Research Center, Texas Agricultural Experiment Station: Temple, TX, USA, 2007; pp. 131–132.*
46. USGS. The National Map—Advanced Viewer. Available online: <https://apps.nationalmap.gov/viewer/> (accessed on 29 January 2021).
47. Duru, U.; Arabi, M.; Wohl, E.E. Modeling stream flow and sediment yield using the SWAT model: A case study of Ankara River Basin, Turkey. *Phys. Geogr.* **2018**, *39*, 264–289. [[CrossRef](#)]
48. Hallouz, F.; Meddi, M.; Mahé, G.; Alirahmani, S.; Keddar, A. Modeling of discharge and sediment transport through the SWAT model in the basin of Harraza (Northwest of Algeria). *Water Sci.* **2018**, *32*, 79–88. [[CrossRef](#)]
49. Al-Khafaji, M.S.; Al-Sweiti, F.H. Integrated Impact of digital elevation model and land cover resolutions on simulated runoff by SWAT model. *Hydrol. Earth Syst. Sci. Discuss.* **2017**, 1–26. [[CrossRef](#)]
50. Al-Khafaji, M.; Saeed, F.H.; Al-Ansari, N. The interactive impact of land cover and DEM Resolution on the accuracy of computed streamflow using the SWAT model. *Water Air Soil Pollut.* **2020**, *231*, 416. [[CrossRef](#)]
51. NRCS. Web Soil Survey—Home. Available online: <https://websoilsurvey.sc.egov.usda.gov/App/HomePage.htm> (accessed on 29 January 2021).

52. National Oceanic and Atmospheric Administration. Available online: <https://www.noaa.gov/> (accessed on 5 February 2021).
53. Essenfelder, A.H. SWAT Weather Database: A Quick Guide; Version V. 0.16; 2016; Volume 6. Available online: https://www.researchgate.net/profile/Arthur-Hrast-Essenfelder-2/publication/330221011_SWAT_Weather_Database_A_Quick_Guide/links/5c34a39192851c22a363cbb0/SWAT-Weather-Database-A-Quick-Guide.pdf (accessed on 5 February 2021).
54. TAMU. Global Weather Data for SWAT. Available online: <https://globalweather.tamu.edu/> (accessed on 5 February 2021).
55. MSU; MAFES. MAFES—Variety Trials. Available online: <https://www.mafes.msstate.edu/variety-trials/includes/forage/about.asp> (accessed on 20 May 2021).
56. USGS. USGS Water Data for the Nation. Available online: <https://waterdata.usgs.gov/nwis> (accessed on 25 February 2021).
57. Abbaspour, K.C. SWAT-CUP-2012. *SWAT Calibration and Uncertainty Program—A User Manual*; Swiss Federal Institute of Aquatic Science and Technology: Dübendorf, Switzerland, 2013.
58. Krause, P.; Boyle, D.P.; Bäse, F. Comparison of different efficiency criteria for hydrological model assessment. *Adv. Geosci.* **2005**, *5*, 89–97. [[CrossRef](#)]
59. Nash, J.E.; Sutcliffe, J.V. River flow forecasting through conceptual models part I—A discussion of principles. *J. Hydrol.* **1970**, *10*, 282–290. [[CrossRef](#)]
60. Runkel, R.L.; Crawford, C.G.; Cohn, T.A. *Load Estimator (LOADEST): A FORTRAN Program for Estimating Constituent Loads in Streams and Rivers*; CreateSpace Independent Publishing Platform: Scotts Valley, CA, USA, 2004. [[CrossRef](#)]
61. White, K.L.; Chaubey, I. Sensitivity analysis, calibration, and validations for a multisite and multivariable SWAT model 1. *J. Am. Water Resour. Assoc.* **2005**, *41*, 1077–1089. [[CrossRef](#)]
62. Cibir, R.; Sudheer, K.P.; Chaubey, I. Sensitivity and identifiability of stream flow generation parameters of the SWAT model. *Hydrol. Process. Int. J.* **2010**, *24*, 1133–1148. [[CrossRef](#)]
63. Brighenti, T.M.; Bonumá, N.B.; Grison, F.; de Almeida Mota, A.; Kobiyama, M.; Chaffe, P.L.B. Two Calibration methods for modeling streamflow and suspended sediment with the SWAT model. *Ecol. Eng.* **2019**, *127*, 103–113. [[CrossRef](#)]
64. Park, Y.S.; Engel, B.A. Use of pollutant load regression models with various sampling frequencies for annual load estimation. *Water* **2014**, *6*, 1685–1697. [[CrossRef](#)]
65. Park, Y.S. Development and Enhancement of Web-Based Tools to Develop Total Maximum Daily Load. Ph.D. Dissertation, Purdue University, Ann Arbor, MI, USA, 2014.
66. Donato, M.M.; MacCoy, D.E. *Phosphorus and Suspended Sediment Load Estimates for the Lower Boise River, Idaho, 1994–2002*; US Department of the Interior, US Geological Survey: Reston, VA, USA, 2005.
67. Lewis, T.; Lamoureux, S.F. Twenty-First century discharge and sediment yield predictions in a small high Arctic watershed. *Glob. Planet. Change* **2010**, *71*, 27–41. [[CrossRef](#)]
68. Waidler, D.; White, M.; Steglich, E.; Wang, S.; Williams, J.; Jones, C.A.; Srinivasan, R. *Conservation Practice Modeling Guide for SWAT and APEX*; Texas A&M University: College Station, TX, USA, 2011. Available online: <https://hdl.handle.net/1969.1/94928> (accessed on 20 February 2022).
69. Arnold, J.G.; Kiniry, J.R.; Srinivasan, R.; Williams, J.R.; Haney, E.B.; Neitsch, S.L. *SWAT 2012 Input/Output Documentation*; Texas Water Resources Institute: College Station, TX, USA, 2013; pp. 494–495.
70. Liu, Y.; Wang, R.; Guo, T.; Engel, B.A.; Flanagan, D.C.; Lee, J.G.; Li, S.; Pijanowski, B.C.; Collingsworth, P.D.; Wallace, C.W. Evaluating efficiencies and cost-effectiveness of best management practices in improving agricultural water quality using integrated SWAT and cost evaluation tool. *J. Hydrol.* **2019**, *577*, 123965. [[CrossRef](#)]
71. Leh, M.D.K.; Sharpely, A.N.; Singh, G.; Matlock, M.D. Assessing the impact of the MRBI program in a data limited Arkansas watershed using the SWAT model. *Agric. Water Manag.* **2018**, *202*, 202–219. [[CrossRef](#)]
72. Wang, L. Evaluation of Vegetated Filter Strip Implementations in Deep River Portage-Burns Waterway Watershed Using SWAT Model. Master’s Thesis, Purdue University, Indiana, IN, USA, 2018.
73. Abimbola, O.; Mittelstet, A.; Messer, T.; Berry, E.; van Griensven, A. Modeling and Prioritizing interventions using pollution hotspots for reducing nutrients, atrazine and e. coli concentrations in a watershed. *Sustainability* **2021**, *13*, 103. [[CrossRef](#)]
74. Moriasi, D.N.; Gitau, M.W.; Pai, N.; Daggupati, P. Hydrologic and water quality models: Performance Measures and evaluation criteria. *Trans. ASABE* **2015**, *58*, 1763–1785. [[CrossRef](#)]
75. Gassman, P.W.; Reyes, M.R.; Green, C.H.; Arnold, J.G. The soil and water assessment tool: Historical development, applications, and future research directions. *Trans. ASABE* **2007**, *50*, 1211–1250. [[CrossRef](#)]
76. Chu, T.W.; Shirmohammadi, A.; Montas, H.; Sadeghi, A. Evaluation of the SWAT Model’s sediment and nutrient components in the piedmont physiographic region of Maryland. *Trans. ASAE* **2004**, *47*, 1523. [[CrossRef](#)]
77. Gikas, G.D.; Yiannakopoulou, T.; Tsihrintzis, V.A. Modeling of Non-point source pollution in a mediterranean drainage basin. *Environ. Model. Assess.* **2006**, *11*, 219–233. [[CrossRef](#)]
78. Tuppard, P.; Kannan, N.; Srinivasan, R.; Rossi, C.G.; Arnold, J.G. Simulation of agricultural management alternatives for watershed protection. *Water Resour. Manag.* **2010**, *24*, 3115–3144. [[CrossRef](#)]
79. Risal, A.; Parajuli, P.B. Evaluation of the impact of best management practices on streamflow, sediment and nutrient yield at field and watershed scales. *Water Resour. Manag.* **2022**, *36*, 1093–1105. [[CrossRef](#)]
80. Mwangi, H.M.; Gathenya, J.M.; Mati, B.M.; Mwangi, J.K. Evaluation of agricultural conservation practices on ecosystem services in Sasumua Watershed, Kenya using SWAT model. *Sci. Conf. Proc.* 2013. Available online: <http://41.204.187.99/index.php/jscp/article/download/861/770> (accessed on 5 March 2022).

81. Jang, S.S.; Ahn, S.R.; Kim, S.J. Evaluation of executable best management practices in Haean highland agricultural catchment of South Korea using SWAT. *Agric. Water Manag.* **2017**, *180*, 224–234. [[CrossRef](#)]
82. Tuppad, P.; Santhi, C.; Srinivasan, R.; Williams, J.R. *Best Management Practice (BMP) verification Using Observed Water Quality Data and Watershed Planning for Implementation of BMPs*; TSSWCB Project 04-I8; Texas A&M AgriLIFE Research: College Station, TX, USA, 2009.